PHYSICAL REVIEW D **80,** 126015 (2009)

Pomeron contribution to pp and $p\bar{p}$ scattering in AdS/QCD

Sophia K. Domokos, Jeffrey A. Harvey, and Nelia Mann

Enrico Fermi Institute and Department of Physics, University of Chicago, Chicago Illinois 60637, USA

(Received 4 August 2009; published 21 December 2009)

We consider the differential and total cross sections for proton-proton and proton-antiproton scattering in the Regge regime from the point of view of string dual models of QCD. We argue that the form factor which appears in the differential cross section is related to the matrix element of the stress tensor between proton states and give a procedure for computing the strength of the coupling of the Pomeron trajectory to the proton. We compute this coupling in the Sakai-Sugimoto model and find excellent agreement with the data at large s and small t. The form factor can be estimated in the Skyrme model or in AdS/QCD models and gives a stiffer form factor than the commonly used electromagnetic form factor, in agreement with our fits to data. Our model is also in good agreement with the measured ratio of real to imaginary parts of the forward scattering amplitude at large s.

DOI: 10.1103/PhysRevD.80.126015 PACS numbers: 11.25.Tq, 11.15.Pg, 11.55.Jy, 13.85.Lg

I. INTRODUCTION

In recent years, holographic QCD (hQCD) models based on the AdS/CFT correspondence have developed as a useful framework for understanding the structure of strongly coupled QCD. They have proved remarkably successful in reproducing meson masses, decay constants, and couplings. The difficulty of performing string calculations on curved backgrounds has largely limited their application to low-energy processes which can be studied in the supergravity limit of the string dual. However, such interesting (and experimentally relevant) processes as the high-energy scattering of hadrons lie outside this limit. In particular, at large center of mass energy $\sqrt{s}$ and small momentum transfer t, perturbative QCD fails—but considering the exchange of only the lowest energy confined states in the supergravity limit of hQCD is also insufficient. Instead, one should include the full tower of higher spin string excitations having the appropriate charge and parity. In this paper, we propose a technique inspired by Regge theory and the structure of string scattering amplitudes to model the high s, low t limit of proton-proton and proton-antiproton scattering.

The outline of this paper is as follows. In Sec. II we review the connection between Regge theory and string theory and discuss the AdS/QCD interpretation of the Pomeron. In Sec. III we use the structure of QCD string duals to develop a model for pp or $p\bar{p}$ elastic scattering in the Regge limit. This model depends on four parameters: the slope and intercept of the Pomeron trajectory, the strength of the coupling of the Pomeron to the proton, and a mass scale which determines the relevant proton form factor. In Sec. IV we compute the mass scale, the Pomeron-proton coupling, and the mass of the lowest particle on the trajectory, in the Sakai-Sugimoto model. In Sec. V we fit our model to data and compare the fit values of the parameters with the computed values. In Sec. VI we conclude and discuss some directions for future research.

II. REGGE THEORY, STRING THEORY, AND THE POMERON

In this section we discuss some of the connections between Regge theory and string theory. While all of the results are known, we hope that this quick summary proves useful to string theorists unfamiliar with Regge theory and to experts on Regge theory who may not have kept up with the latest developments in string theory and AdS/QCD. It will also serve to establish some of our key assumptions and to compare them with some of the phenomenological literature on Pomeron exchange. While Regge theory can certainly be constructed independently of string theory, many of its results are more easily understood from a string-theoretic point of view; the Regge behavior of hadronic processes also hints strongly at the existence of a string dual description of QCD. As we will see, string duals of QCD illuminate some aspects of Regge theory which in the past were determined purely phenomenologically.

We are concerned, in particular, with the forward behavior of proton-proton or proton-antiproton scattering. In the Regge limit of small t and large s, the total cross section, the differential cross section, and the ρ parameter are given in terms of the invariant scattering amplitude ($\mathcal{A}^{pp}(s,t)$ or $\mathcal{A}^{p\bar{p}}(s,t)$) [1] as

$$\sigma_{\rm tot} = \frac{1}{s}\,{\rm Im}\mathcal{A}(s,0), \qquad \frac{d\sigma}{dt} = \frac{1}{16\pi s^2}|\mathcal{A}(s,t)|^2, \qquad \rho(s) = \frac{{\rm Re}\mathcal{A}(s,0)}{{\rm Im}\mathcal{A}(s,0)}. \tag{1}$$

QCD is strongly coupled in this regime, so a perturbative expansion in the QCD coupling cannot be used to compute these quantities. It is natural, then, to try to compute them in the $1/N_c$ expansion, which often provides insight into the properties of QCD when standard perturbation theory fails [2,3]. At large N_c, the QCD spectrum includes infinite towers of narrow mesons and glueballs with arbitrarily high spin. For example, it is easy to construct gauge

invariant operators with spin J which have the same quantum numbers as the ω meson. These operators create higher mass and spin versions of the ω, which also have nonzero couplings to baryons. Since the effective coupling between mesons is $g_{\rm eff} \sim 1/\sqrt{N_c}$, these states become arbitrarily narrow as $N_c \to \infty$. Tree-level t-channel exchange of such a spin J meson implies an amplitude which behaves as s^J. Naively, terms with larger J become more important at large s; the sum over all such exchanges would then lead to amplitudes which grow rapidly at large s, violating the requirements of unitarity.

Regge theory instead sums up these exchanges of particles with fixed quantum numbers and higher mass and spin (Regge trajectories) into a form that can be associated with a t-dependent pole at $J = \alpha(t)$ in the complex angular momentum plane [4]. There is a great deal of evidence that these Regge trajectories are well-approximated by a linear function, $\alpha(t) = \alpha(0) + \alpha' t$. At positive t (corresponding to the crossed channel for a $2 \to 2$ scattering process) this is evidenced by the fact that mesons can indeed be arranged into groups with $J = \alpha(0) + \alpha' M^2$. For example, the trajectory which includes the $I = 1$ mesons ρ, a_2, ρ_3, a_4 has $\alpha(0) \sim 0.53$ and $\alpha' \sim 0.88$ GeV^{-2}. At small negative t, one can extract $\alpha(t)$ from the differential cross section, which in Regge theory has the characteristic form

$$\frac{d\sigma}{dt} = \beta(t)\left(\frac{s}{s_0}\right)^{2\alpha(t)-2}. \tag{2}$$

Data from a variety of scattering processes show that the linearity of trajectories extends to moderate values of negative t with the same slope and intercept as at positive t. While there is evidence that more complicated singularities are also required to describe the full range of hadronic data (e.g. Regge cuts) the basic picture of exchange of single Regge poles accounts for the structure of many hadronic scattering processes in the Regge limit.

High-energy total cross section data quickly make it clear, however, that a theory based purely on the exchange of known meson states is not sufficient to describe the scattering of hadrons. The Regge behavior described above leads to total cross sections $\sigma_{\rm tot} \propto (\mathrm{Im}\mathcal{A}(s,0))/s$ which behave as $s^{\alpha(0)-1}$ at large s. Since all the known meson Regge trajectories have intercepts $\alpha(0) \leq 0.6$, they cannot explain the experimental fact that total cross sections for hadronic processes tend to grow very slowly with increasing s, at a rate independent of the quantum numbers of the scattered particles. This was apparent even in the early 1960s, and led [5,6] to propose the existence of a new Regge trajectory dubbed the ''Pomeron,'' with even signature, vacuum quantum numbers, and intercept $\alpha_{\mathcal{P}}(0) \sim 1$, that governed the large s behavior of total cross sections. There have been many attempts over the years to fit total cross sections with a combination of Reggeon and Pomeron contributions. See for example [7,8], both of which conclude that the Pomeron has an intercept $\alpha_{\mathcal{P}}(0) \sim 1.06$–$1.08$ and a slope $\alpha'_{\mathcal{P}} \sim 0.25$ GeV^{-2}.

However, the existence of the Pomeron trajectory and its structure has remained elusive for a number of reasons. First of all, it is not easy to identify the corresponding trajectory at positive t, though many candidate states with the correct quantum numbers do exist. It is not even clear that the Pomeron trajectory is unique. One could certainly imagine that there are several Pomeron trajectories, just as there are a variety of Reggeon trajectories. Second, the $s^{0.08}$ growth of total cross sections implied by fits to the Pomeron intercept eventually violates the Froissart-Martin bound, which requires that total cross sections grow no faster than $\log^2 s$ as $s \to \infty$. Thus single Pomeron exchange cannot be the full story for sufficiently high s. Whether we have already reached a value of s where such effects must be included is quite controversial. Attempts to test the question of single Pomeron exchange versus unitarized models of multi-Pomeron exchange (or extrapolations of perturbative QCD using fits to forward data) have unfortunately led to inconclusive results [9]. Finally, at increasing $|t|$ one encounters features in the data which are not easily described by single Pomeron exchange with the same trajectory as at small $|t|$. This has led to the idea of a ''hard Pomeron'' which in some papers is treated as a separate trajectory and in others is viewed as a change in the behavior of a single trajectory as $|t|$ increases.

String dual models of QCD [10–13] which grew out of the AdS/CFT correspondence [14–16] have shed some light on these issues [17]. In hQCD, meson states are dual to open strings and glueball states to closed strings. Analysis of the glueball spectrum in string duals [18] as well as lattice gauge theory studies [19] support the idea that there is a single Pomeron trajectory consisting of glueball states, with the lowest mass state on the leading trajectory being a 2^{++} state and with the lowest mass 0^{++} state lying on a ''daughter trajectory'' (a trajectory having the same quantum numbers as the ''leading'' trajectory, but a smaller intercept). The analysis of [17] also establishes a connection between the soft Pomeron and the hard Balitsky-Fadin-Kuraev-Lipatov Pomeron, which emerges from perturbative QCD [20]. For theories like QCD, which exhibit confinement and logarithmic running couplings, it leads to a theory where a discrete spectrum of poles at positive t evolves continuously into a set of closely spaced poles on a flatter trajectory (see e.g. Fig. 11 in [17]). The transition between these two behaviors is expected to occur at scales of order $\Lambda_{\rm QCD}$. This picture very closely resembles one which emerges from models which generically use a fifth dimension, r, to encode the energy scale of the theory, and thus the running of the string tension [21]. The full amplitude therefore becomes a sum over densely spaced trajectories with $\alpha(0)$ and α' depending on the energy scale r, so that a different trajectory dominates at

each value of t. Analyzing the Veneziano and Virasoro-Shapiro amplitudes in this context (see e.g. [22,23]) reveals a similar dependence of the trajectory slopes to that found in [17]. Unfortunately, the region of most interest for our analysis, $-\Lambda_{\rm QCD}^2 < t \leq 0$, appears to be extremely model-dependent and difficult to analyze in all such models. Based on the picture outlined above, we will assume that there is a single Pomeron trajectory and focus entirely on the regime in which this trajectory promises to dominate. We also assume that one of the primary effects of the curved space background in AdS duals is to shift the slope and the intercept of the leading closed string Regge trajectory from their flat space values. Computing this shift in the region of most phenomenological interest is a difficult problem. For various approaches see [17,24]. We will later present an analysis of the effective trajectory extracted from data that suggests a linear trajectory in the region $-0.6\ {\rm GeV}^2 < t \leq 0$, and will fit its slope and intercept.

We now review how the most important elements of Regge theory indeed emerge from string amplitudes. Here we consider only flat space amplitudes, which are sufficient to illustrate Regge behavior. In the next section we will assume that amplitudes in curved space retain much of this structure but with shifted values for the parameters of the Regge trajectory.

Let us begin with an amplitude for open string exchange, which should correspond to the exchange of Reggeons. The Veneziano amplitude, first introduced as a model for $\pi + \pi \rightarrow \omega + \pi$ scattering, and later recognized as defining open string scattering, can be written in terms of the amplitude

$$\mathcal{A}^{\rm Ven}_{\{n,m,p\}}(s,t) = \frac{\Gamma[n - a_o(s)]\Gamma[m - a_o(t)]}{\Gamma[p - a_o(s) - a_o(t)]}. \tag{3}$$

The crossing symmetric combination appearing in Veneziano's original paper [25] is

$$\mathcal{A}^{\rm Ven}_{\{1,1,2\}}(s,t) + \mathcal{A}^{\rm Ven}_{\{1,1,2\}}(t,u) + \mathcal{A}^{\rm Ven}_{\{1,1,2\}}(s,u), \tag{4}$$

while the open bosonic string four-tachyon amplitude is simply

$$\mathcal{A}_o(p_1,p_2,p_3,p_4) \propto \mathcal{A}^{\rm Ven}_{\{0,0,0\}}(s,t) + \mathcal{A}^{\rm Ven}_{\{0,0,0\}}(u,t) + \mathcal{A}^{\rm Ven}_{\{0,0,0\}}(s,u), \tag{5}$$

where we have ignored Chan-Paton factors and an overall constant. In the above we take $a_o(x)$ to be a linear function: $a_o(x) = a_o(0) + a_o' x$. To avoid notational confusion later on, we use $a_o(x)$ and $a_c(x)$ for the linear functions which appear in open and closed string amplitudes and reserve the notation $\alpha(0)$ and α' for the intercept and slope of the straight line relating J to M^2 on a Regge trajectory. Thus for closed string Regge trajectories we have $J = \alpha_c(0) + \alpha_c' M^2$ and we define $\alpha_c(x) = \alpha_c(0) + \alpha_c' x$. This will become clearer in the following when we contrast the Regge limits of open and closed string amplitudes.

In the Regge limit ($s \rightarrow +\infty$ and t fixed), the Veneziano amplitude does not behave smoothly: it has poles for large, positive, real s. This can be remedied by giving s a small imaginary part, which corresponds physically to giving the meson states a small width, thus moving their poles slightly off the real axis. One finds that for large, complex s

$$\mathcal{A}^{\rm Ven}_{\{0,0,0\}}(s,t) \rightarrow (-a_o' s)^{a_o(t)}\Gamma[-a_o(t)] = e^{-i\pi a_o(t)}(a_o' s)^{a_o(t)}\Gamma[-a_o(t)], \tag{6}$$

$$\mathcal{A}^{\rm Ven}_{\{0,0,0\}}(u,t) \rightarrow (a_o' s)^{a_o(t)}\Gamma[-a_o(t)] \tag{7}$$

(using $u \sim -s$ in the Regge limit), and that $\mathcal{A}_0^{\rm Ven}(u,s)$, which does not have any t-channel poles, vanishes exponentially in s in this limit. From this we can easily see that the open string amplitude explicitly reproduces the Regge form of the differential cross section in (2).

The linear combinations of amplitudes which are even or odd under the exchange $u \rightarrow s$ have Regge limits

$$\begin{aligned} \mathcal{A}_o^+ &\equiv \mathcal{A}^{\rm Ven}_{\{0,0,0\}}(s,t) + \mathcal{A}^{\rm Ven}_{\{0,0,0\}}(u,t) \\ &\rightarrow (1 + e^{-i\pi a_o(t)})(a_o' s)^{a_o(t)}\Gamma[-a_o(t)] \\ \mathcal{A}_o^- &\equiv \mathcal{A}^{\rm Ven}_{\{0,0,0\}}(s,t) - \mathcal{A}^{\rm Ven}_{\{0,0,0\}}(u,t) \\ &\rightarrow (-1 + e^{-i\pi a_o(t)})(a_o' s)^{a_o(t)}\Gamma[-a_o(t)]. \end{aligned} \tag{8}$$

The prefactors in parentheses are known in Regge theory as "signature factors" and have zeroes when $a_o(t)$ is an odd integer in $\mathcal{A}_o^+$ or an even integer in $\mathcal{A}_o^-$. Using the product formula

$$\Gamma[-a_o(t)] = \frac{e^{\gamma a_o(t)}}{a_o(t)} \prod_{n=1}^{\infty} \frac{n e^{-a_o(t)/n}}{(a_o(t) - n)}, \tag{9}$$

we see that $\mathcal{A}_o^+$ has poles at $a_o(t) = 2k$ with residue $\sim s^{2k}$ for k a nonnegative integer. Thus $\mathcal{A}_o^+$ corresponds to the exchange of a Regge trajectory of particles with even integer spin. Similarly, $\mathcal{A}_o^-$ corresponds to exchange of a Regge trajectory with odd integer spin. Since in either case we find the angular momentum of the particles being exchanged near a t-channel pole is $J = \alpha(t)$, for the open string we can identify $a_o' = \alpha_o'$ and $a_o(0) = \alpha_o(0)$ and thus $a_o(t) = \alpha_o(t)$. When one considers the scattering of string states with higher spin, or extends the bosonic string to the superstring, the general structure of tree-level amplitudes in terms of ratios of gamma functions remains the same, the only difference being the addition of a kinematic factor $K_o(1,2,3,4)$ which depends on the polarization tensors or spinor structures of the scattered particles and their momenta. This implies that the higher mass and spin states being exchanged have couplings and vertex factors tightly constrained by duality in terms of the couplings and vertex factors of the lightest exchanged states.

We have now seen that the open (bosonic) string amplitude exhibits the correct pole and residue structure to reproduce the form of the phenomenological Regge am-

plitude, and also naturally includes signature factors for exchange of resonances with even or odd spin. Of course, the open bosonic string amplitude has obvious problems as a candidate for describing scattering of mesons. In particular, the ground state, corresponding to the first pole of $\mathcal{A}_o^+$, is a tachyon and the first spin 1 state exchanged in $\mathcal{A}_o^-$ is a massless gauge field. However, one can easily modify the string theory amplitude for phenomenological purposes [26,27] by using $\mathcal{A}^{\rm Ven}_{\{1,1,1\}}$ instead of $\mathcal{A}^{\rm Ven}_{\{0,0,0\}}$ and by using the phenomenologically determined values of the slope and intercept for meson trajectories.

Let us now turn to closed string scattering, dual to the exchange of a trajectory of glueball states (i.e. the Pomeron). The simplest example is the scattering in flat space of four closed string tachyons, given by the Virasoro-Shapiro amplitude

$$\mathcal{A}_c(p_1, p_2, p_3, p_4) = \frac{\Gamma[-a_c(s)]\Gamma[-a_c(t)]\Gamma[-a_c(u)]}{\Gamma[-a_c(t) - a_c(s)]\Gamma[-a_c(t) - a_c(u)]\Gamma[-a_c(u) - a_c(s)]}. \tag{10}$$

When we use this amplitude for phenomenological purposes we will include a kinematic prefactor $K_c(1, 2, 3, 4)$ and fit the slope and intercept to data rather using the values from the critical bosonic string.

To take the Regge limit it is useful to write the u dependence in terms of s and t. For the simplest case of $2 \to 2$ scattering of particles with equal mass m we have

$$a_c(s) + a_c(t) + a_c(u) = 4a_c' m^2 + 3a_c(0) \equiv \chi \tag{11}$$

so that

$$\mathcal{A}_c(p_1, p_2, p_3, p_4) = \frac{\Gamma[-a_c(s)]\Gamma[-a_c(t)]\Gamma[a_c(s) + a_c(t) - \chi]}{\Gamma[-a_c(t) - a_c(s)]\Gamma[a_c(t) - \chi]\Gamma[a_c(s) - \chi]}. \tag{12}$$

Then, using the limits

$$\frac{\Gamma[-a_c(s)]}{\Gamma[-a_c(s) - a_c(t)]} \to (-a_c' s)^{a_c(t)}, \tag{13}$$

and

$$\frac{\Gamma[a_c(s) + a_c(t) - \chi]}{\Gamma[a_c(s) - \chi]} \to (a_c' s)^{a_c(t)}, \tag{14}$$

we have the Regge limit of the Virasoro-Shapiro amplitude

$$\mathcal{A}_c^{\rm Reg}(p_1, p_2, p_3, p_4) = e^{-i\pi a_c(t)}(a_c' s)^{2a_c(t)} \frac{\Gamma[-a_c(t)]}{\Gamma[a_c(t) - \chi]}. \tag{15}$$

This amplitude has poles at $a_c(t) = n$ for $n = 0, 1, 2, \ldots$ with residue $\sim s^{2n}$. This corresponds to t-channel exchange of a Regge trajectory with $J = 2n = 0, 2, 4, \ldots$. Note that it is not necessary to do any projection or add amplitudes to get exchange of only even J poles; this arises as a consequence of the fact that the leading closed string Regge trajectory contains only even spin states. We also note that $J = 2a_c(t)$, implying that $\alpha_c' = 2a_c'$ and $\alpha_c(0) = 2a_c(0)$.

The above discussion suggests two possible amplitudes to describe the exchange of an even signature Regge trajectory whose lowest state has spin $J_0 = 2$: (1) the Regge limit of either the even signature part of the Veneziano amplitude for open string theory or (2) the Regge limit of the Virasoro-Shapiro amplitude for closed string theory. Rewritten in terms of the actual Regge trajectories $\alpha_o(t)$ and $\alpha_c(t)$, including the kinematic prefactor, they are

$$\mathcal{A}_o^{\rm Reg}(s, t) = [K_o(1, 2, 3, 4)(\alpha_o' s)^{-2}]e^{-i\pi\alpha_o(t)/2}2 \times \cos(\pi\alpha_o(t)/2)(\alpha_o' s)^{\alpha_o(t)}\Gamma(2 - \alpha_o(t)), \tag{16}$$

and

$$\mathcal{A}_c^{\rm Reg}(s, t) = [K_c(1, 2, 3, 4)(\alpha_c' s/2)^{-2}] \times e^{-i\pi\alpha_c(t)/2}(\alpha_c' s/2)^{\alpha_c(t)} \frac{\Gamma(1 - \alpha_c(t)/2)}{\Gamma[\alpha_c(t)/2 - 1 - \chi]}. \tag{17}$$

By assumption the factor in square brackets approaches a constant at large s.

The total cross section and the parameter $\rho = \mathrm{Re}\mathcal{A}(s, 0)/\mathrm{Im}\mathcal{A}(s, 0)$ are identical in either case. Provided the same Regge trajectory is used, they differ only by an overall constant at $t = 0$. However, the amplitudes do predict distinct differential cross sections as these involve behavior at nonzero t. Regge amplitudes are often written in the form $(s/s_0)^{\alpha(t)}$ and we see that the reference scale s_0 differs in the two amplitudes. They also differ in their t dependence with the most dramatic difference being the existence of zeroes in the open string amplitude at $\alpha_o(t) = -1, -3, -5, \ldots$ (these are often called EXD [exchange degenerate] zeroes in the literature and arise from the need to project out the even spin states from an exchange degenerate trajectory with both even and odd spins)

while the closed string amplitude has zeroes coming from the poles in the denominator at $\alpha_c(t) = 2\chi + 2$, $2\chi, 2\chi - 2, \ldots$.

In the application of this formalism to proton-proton scattering discussed in the following section we use the closed string amplitude to model Pomeron exchange, since the Pomeron trajectory is a closed string trajectory in holographic duals of QCD. The situation is a bit murky, however. In dual models the proton is neither an open string nor a closed string but rather a solitonic excitation of open strings (as expected from large N_c reasoning [28]), so while the exchanged states are indeed closed strings, the states being scattered are not.

III. A GENERAL MODEL FOR pp ELASTIC SCATTERING IN THE REGGE REGIME

We now use the behavior of the string amplitudes sketched above to develop a method for computing proton-proton scattering in a holographic string dual of QCD. One should note that at present all the proposed duals have serious limitations; we also lack the technical tools to calculate the full tree-level string amplitudes in a curved space background, which should actually govern the behavior of proton-proton scattering. As a result we will have to make certain approximations. Our first assumption (consistent with factorization in Regge theory) is that we can split the calculation into two parts. (1) We determine the vertex which governs the coupling of the Pomeron to the proton, which we assume is dictated by the vertex for the lowest state on the Pomeron trajectory, the 2^{++} glueball. Using this vertex, we compute the amplitude for tree-level exchange of a spin 2 glueball. (2) We then convert this amplitude into the Regge limit of a full tree-level string amplitude by "Reggeizing" the propagator. This is a heuristic procedure, described in detail below, which gives an answer consistent with the general principles of Regge theory. It should be a good starting approximation if the main effect of curved space and background fields on the string theory is to shift the slope and intercept of the Regge trajectory from their flat space values.

A. The glueball coupling

Our first task is to determine the coupling of the glueball field to the proton. The glueball field can be treated as a second-rank symmetric traceless tensor $h_{\mu\nu}$. Old ideas of tensor-meson dominance, [29,30] applied now to the 2^{++} glueball rather than to the f_2 meson, suggest that $h_{\mu\nu}$ should couple predominantly to the QCD stress tensor $T^{\mu\nu}$:

$$S_{\rm int} = \lambda \int d^4x h_{\mu\nu} T^{\mu\nu}. \tag{18}$$

Assuming this is true, the glueball-proton-proton vertex is determined by the matrix element of the stress tensor between proton states

$$\langle p', s'|T_{\mu\nu}(0)|p, s\rangle. \tag{19}$$

Using symmetry and conservation of $T_{\mu\nu}$ this matrix element can be written in terms of three form factors [31] as

$$\begin{aligned}\langle p', s'|T_{\mu\nu}(0)|p, s\rangle = \bar{u}(p', s')\Big[A(t)\frac{\gamma_\alpha P_\beta + \gamma_\beta P_\alpha}{2} \\ + B(t)\frac{i(P_\alpha\sigma_{\beta\rho} + P_\beta\sigma_{\alpha\rho})k^\rho}{4m_p} \\ + C(t)\frac{(k_\alpha k_\beta - \eta_{\alpha\beta}k^2)}{m_p}\Big]u(p, s),\end{aligned} \tag{20}$$

where $k = p' - p'$, $t = k^2$, and $P = (p + p')/2$. The fact that the proton has spin $1/2$ and mass m_p implies the constraints $A(0) = 1$ and $B(0) = 0$. We will see in the following subsection that the contribution from $C(t)$ is suppressed in the Regge limit and that the contribution from $B(t)$ is small compared to that from $A(t)$. We note that gravitational form factors of nucleons have been studied in the holographic context in [32] and also play an important role in the analysis of deeply virtual Compton scattering [33]; for our purposes, however, a simple analysis of their behavior in the Regge limit will suffice.

How are the two ingredients—the glueball and the proton—manifest in a string dual description? Any hQCD model necessarily involves a theory containing gravity in a five-dimensional space (often along with additional compact directions), where one of the coordinates is dual to the energy scale of QCD. There is therefore inevitably a graviton, which gives rise to a mode transforming as the desired 2^{++} glueball field. In order to have dynamical mesons and baryons (rather than just a baryon vertex as in [34]) there must also be fields in the theory which are dual to operators constructed out of quark fields. In particular, there must be a gauge field dual to the axial-vector current operator which creates pions in QCD. In the large N_c limit of QCD baryons may be treated as Skyrmions, that is as solitons of the pion field. Dual models lend themselves to this interpretation of baryons as Skyrmions, though we could also contemplate adding in fields dual to baryon operators in QCD, as suggested in the recent work of [35].

Fluctuations h_{MN} of the five-dimensional background metric by definition couple to the five-dimensional stress tensor for the matter fields via

$$\frac{1}{2}\int d^5x\sqrt{g}T^{\rm matter}_{MN}h^{MN}, \tag{21}$$

where $T^{\rm matter}_{MN}$ includes a contribution from the fields which are dual to the pion. In this case, T_{MN} is the energy-momentum tensor on a solitonic solution representing the proton. To reduce this to a four-dimensional coupling of the glueball we expand the spin 2 piece of the metric

perturbation $h^{\mu\nu}$ in terms of the glueball wave function, and the matter fields in terms of the four-dimensional pion and vector meson fields. There is no guarantee that this will yield a four-dimensional coupling of the glueball predominantly to the four-dimensional stress tensor of the proton. However, analogy to similar results for vector meson dominance in dual models [36,37] leads us to believe that this is indeed the case, and we show by explicit calculation that this is true in the Sakai-Sugimoto model. Making this assumption, then, we can evaluate the coupling λ as an overlap integral of pion and glueball wave functions.

Given a semiclassical solution representing a baryon it is then straightforward following the discussion in [38] to compute the relevant form factors. We should note that we are computing this vertex in the large N_c limit. On the dual string theory side, this is a classical limit with the string coupling $g_s \to 0$, so the calculation can be done in terms of a semiclassical solution to the equations of motion.

B. Tree-level glueball exchange

Let us now use the generic form of the vertex discussed in the previous section to calculate the cross section due to glueball exchange. We will then "Reggeize" the glueball propagator wherever it appears in the amplitude, to include in our model scattering of higher spin glueballs.

Consider a massive, spin 2 glueball exchanged in the t-channel (the dominant channel in the Regge limit). The Feynman diagram for this process is shown in Fig. 1.

We use p_1 and p_2 as incoming momenta and p_3 and p_4 as outgoing momenta, with s, t, and u defined in the usual way, with $k = p_1 - p_3 = p_2 - p_4$ the momentum of the glueball. The massive spin 2 propagator (as given in [39]) is

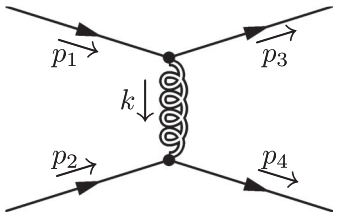

FIG. 1. The Feynman diagram for the exchange of a glueball in the t-channel.

$$\frac{d_{\alpha\beta\gamma\delta}(k)}{k^2 - m_g^2}, \tag{22}$$

where m_g is the mass of the glueball and the indices contracted at one side of the propagator are α, β, the indices at the other end are γ, δ, and

$$\begin{aligned} d_{\alpha\beta\gamma\delta} = {} & \frac{1}{2}(\eta_{\alpha\gamma}\eta_{\beta\delta} + \eta_{\alpha\delta}\eta_{\beta\gamma}) \\ & - \frac{1}{2m_g^2}(k_\alpha k_\delta \eta_{\beta\gamma} + k_\alpha k_\gamma \eta_{\beta\delta} + k_\beta k_\delta \eta_{\alpha\gamma} \\ & + k_\beta k_\gamma \eta_{\alpha\delta}) + \frac{1}{24}\left[\left(\frac{k^2}{m_g^2}\right)^2 - 3\left(\frac{k^2}{m_g^2}\right) - 6\right] \\ & \times \eta_{\alpha\beta}\eta_{\gamma\delta} - \frac{k^2 - 3m_g^2}{6m_g^4}(k_\alpha k_\beta \eta_{\gamma\delta} + k_\gamma k_\delta \eta_{\alpha\beta}) \\ & + \frac{2k_\alpha k_\beta k_\gamma k_\delta}{3m_g^4}. \end{aligned} \tag{23}$$

Using the glueball-proton-proton coupling in the form of Eq. (20) from the previous section, the amplitude becomes

$$\begin{aligned} \mathcal{A} = {} & \frac{\lambda^2 d_{\alpha\beta\gamma\delta}}{t - m_g^2}\left[A(t)(\bar{u}_1\gamma^\alpha u_3)(p_1 + p_3)^\beta + \frac{iB(t)}{2m_p}(p_1 + p_3)^\beta k_\rho(\bar{u}_1\sigma^{\alpha\rho}u_3) + \frac{C(t)}{m_p}(\bar{u}_1 u_3)(k^\alpha k^\beta - \eta^{\alpha\beta}t)\right] \\ & \times\left[A(t)(\bar{u}_2\gamma^\gamma u_4)(p_2 + p_4)^\delta + \frac{iB(t)}{2m_p}(p_2 + p_4)^\delta k_\lambda(\bar{u}_2\sigma^{\gamma\lambda}u_4) + \frac{C(t)}{m_p}(\bar{u}_2 u_4)(k^\gamma k^\delta - \eta^{\gamma\delta}t)\right]. \end{aligned} \tag{24}$$

Using the Dirac equation we can see that

$$k_\mu(\bar{u}_1\gamma^\mu u_3) = k_\mu(\bar{u}_2\gamma^\mu u_4) = 0 \tag{25}$$

and

$$k_\mu(p_1 + p_3)^\mu = k_\mu(p_2 + p_3)^\mu = 0. \tag{26}$$

Furthermore, the second structure in the vertex will vanish when dotted into pairs of k^μ. This means we can ignore all terms in the propagator except those of the form $\eta\eta$. We will be taking the Regge limit of the amplitude, so we can drop any terms that will be suppressed by factors of t/s or m_p^2/s. The amplitude then becomes

$$\mathcal{A} = \frac{\lambda^2}{2(t-m_g^2)}\Big\{2sA^2(t)(\bar{u}_1\gamma^\alpha u_3)(\bar{u}_2\gamma_\alpha u_4) + 4A^2(t)p_2^\alpha p_1^\beta(\bar{u}_1\gamma_\alpha u_3)(\bar{u}_2\gamma_\beta u_4)$$
$$+ \frac{iA(t)B(t)}{2m_p}[2sk^\rho(\bar{u}_1\sigma_{\alpha\rho}u_3)(\bar{u}_2\gamma^\alpha u_4) + 2sk_\lambda(\bar{u}_1\gamma_\gamma u_3)(\bar{u}_2\sigma^{\gamma\lambda}u_4) + 4p_{2\rho}p_{4\alpha}p_1^\beta(\bar{u}_1\sigma^{\alpha\rho}u_3)(\bar{u}_2\gamma_\beta u_4)$$
$$+ 4p_{1\lambda}p_{3\gamma}p_2^\beta(\bar{u}_1\gamma_\beta u_3)(\bar{u}_2\sigma^{\gamma\lambda}u_4)] - \frac{B^2(t)}{4m_p^2}[2sk_\rho k^\lambda(\bar{u}_1\sigma^{\alpha\rho}u_3)(\bar{u}_2\sigma_{\alpha\lambda}u_4) + 4p_{2\rho}p_{4\alpha}p_{1\lambda}p_{3\gamma}(\bar{u}_1\sigma^{\alpha\rho}u_3)(\bar{u}_2\sigma^{\gamma\lambda}u_4)]$$
$$+ \left[\frac{1}{12}\left[\left(\frac{t}{m_g^2}\right)^2 - \frac{3t}{m_g^2} - 6\right]\left(2m_pA(t) + \frac{B(t)t}{2m_p} - \frac{3C(t)t}{m_p}\right)^2 + \frac{2tC(t)}{m_p^2}(3C(t) - tB(t) - 4m_p^2A(t))\right](\bar{u}_1u_3)(\bar{u}_2u_4)\Big\}. \quad (27)$$

The cross section can then be calculated from the amplitude, and it will be proportional to

$$\frac{1}{4}\sum_{\text{spins}}|\mathcal{A}|^2 = \frac{16\lambda^4 s^4}{(t-m_g^2)^2}\left(A^2(t) - \frac{tB^2(t)}{16m_p^2}\right)^2 + \cdots, \quad (28)$$

where we suppress all terms subleading in t/s or m_p^2/s.

The form factor $B(t)$ is zero at $t = 0$ and slowly varying. Together with the factor of $\frac{t}{16m_p^2}$ this implies that at small t, the term proportional to $B^2(t)$ is very small compared to the $A^2(t)$ term. The part of the cross section proportional to $A(t)$ dominates, allowing us to drop all other terms and simply associate a $\lambda A(t)$ to each vertex in the amplitude, giving

$$\frac{d\sigma}{dt} = \frac{\lambda^4 s^2 A^4(t)}{\pi(t-m_g^2)^2} \quad (29)$$

as the cross section for spin 2 glueball exchange. Note that the appearance of s^2 in the numerator is precisely the correct s^J dependence expected from the exchange of a spin 2 particle. The denominator $(t-m_g^2)^2$ will be replaced by the square of the Reggeized propagator we describe in the next subsection.

C. Reggeizing the propagator

Having computed the cross section for exchanging the lightest state on the 2^{++} trajectory, we must include the higher spin states on the trajectory, which correspond to stringy excitations on the curved background. As noted above, the computation of the full string amplitude is prohibitively difficult. Instead, we analyze in greater detail the scattering amplitude for four closed strings in flat space, and from this extract the propagator for a t-channel closed string exchanged in the Regge limit.

As discussed in the previous section, the scattering amplitudes for closed bosonic strings and for closed superstrings take the form

$$\mathcal{A} = \frac{\Gamma[-a(t)]\Gamma[-a_c(u)]\Gamma[-a_c(s)]}{\Gamma[-a_c(t)-a_c(s)]\Gamma[-a_c(t)-a_c(u)]\Gamma[-a_c(u)-a_c(s)]}K_c(p_1, p_2, \ldots), \quad (30)$$

where K_c is a kinematic factor with no poles, which depends on the momenta and polarizations of the scattered particles. $a_c(x)$ is some linear function related to the spectrum of closed strings:

$$a_c(x) = a_c(0) + a_c'x. \quad (31)$$

We assume that this basic form of the amplitude holds true in (weakly) curved space, with $a_c(0)$, a_c', and the kinematic factor K_c undetermined and dependent on the details of the geometrical background. This amplitude boasts many features that are important to modeling Pomeron exchange. For example, it is completely symmetric under the exchanges of s, t, and u. We know experimentally that proton-proton scattering and proton-antiproton scattering have the same behavior in the limit where Pomeron exchange dominates, and we know that crossing symmetry therefore requires that the amplitude be completely symmetric under exchanges of s, t, and u. In addition, the amplitude has the correct pole and residue structure to describe the exchange of even spin, vacuum quantum number states.

To find the proper Reggeized replacement for the spin 2 glueball propagator in (29), we first expand the amplitude around one of the t-channel poles, which occur at $a_c(t) = n$, with $n = 0, 1, 2, \ldots$:

$$\mathcal{A} \approx \frac{(1+a_c(s))\cdots(n+a_c(s))(-\chi+a_c(s))\cdots(-\chi+n-1+a_c(s))}{n!\Gamma[n-\chi](n-a_c(t))}K_c(p_1, p_2, \ldots), \quad (32)$$

where χ is defined as in Eq. (11) and K_c is evaluated at $a_c(t) = n$. As we would expect for the sum of exchanges of all particles on the Regge trajectory, the residue of the pole is a polynomial in s, and we can identify the leading behavior of this polynomial as s^J if the particle being exchanged has spin J. That is

$$\mathcal{A} \approx \frac{P_{2n}(a_c' s)(s^k f(t, \epsilon_i) + \cdots)}{n!\Gamma[n - \chi](n - a_c(t))}, \tag{33}$$

where

$$K_c(p_1, p_2, \ldots) \propto s^k f(\epsilon_i) + \cdots \tag{34}$$

with $f(\epsilon_i)$ some unknown function of the polarizations of the scattered particles which will factor out of our calculation in the end. $P_{2n}(a_c' s)$ is a polynomial of degree $2n$ whose first term is $(a_c' s)^{2n}$. The spin of the nth particle on the trajectory is then

$$J = k + 2n. \tag{35}$$

We can therefore use the leading s behavior of the kinematic factor K_c to arrange the spin of the lowest particle on the trajectory to be whatever we want, after which the higher spins are completely determined. In our case, the $n = 0$ pole should correspond to a spin 2 particle, meaning that $k = 2$. This implies that the trajectory of particles contributing to the amplitude in the Regge limit (where s is large) consists only of even spin particles, consistent with the Pomeron coupling identically to particles and their antiparticles. When we assume that the Pomeron is the dual of a closed string, this comes about quite naturally. By contrast, if we had assumed that the Pomeron is dual to an open string, we would have used the Veneziano amplitude, which has poles for both even and odd spin particles.

Let us now relate our string amplitude parameters $a_c(0)$ and a_c' to the traditional parameters of Regge theory. If we have

$$\alpha_c(0) + \alpha_c' m_J^2 = J \tag{36}$$

and $J = 2n + 2$, then we need

$$2a_c(0) + 2 = \alpha_c(0), \quad \text{and} \quad 2a_c' = \alpha_c'. \tag{37}$$

In the Regge limit (where we keep only the leading s behavior), the amplitude from the exchange of the lowest particle on the trajectory will simply be

$$\mathcal{A} \approx \frac{-s^2 f(\epsilon_i)}{a_c' \Gamma[-\chi](t - m_g^2)}, \tag{38}$$

where we have used the fact that the mass of the lowest particle on the trajectory (the spin 2 particle) is

$$m_g^2 = m_2^2 = -\frac{a_c(0)}{a_c'}. \tag{39}$$

If we take the Regge limit of the full amplitude, however, we find

$$\mathcal{A} \to \frac{\Gamma[1 - \frac{\alpha_c(t)}{2}]}{\Gamma[\frac{\alpha_c(t)}{2} - 1 - \chi]} e^{-i\pi\alpha_c(t)/2} \left(\frac{\alpha_c' s}{2}\right)^{\alpha_c(t)-2} s^2 f(\epsilon_i) \tag{40}$$

(where we are now using the characteristic parameters $\alpha_c(0)$, α_c' of the Regge trajectory). Note again that the factor $f(\epsilon_i)$ contains all information about the incoming and outgoing particles. We can thus relate this amplitude to the amplitude in Eq. (38) by replacing the glueball exchange factor $\frac{1}{t - m_g^2}$ with a Reggeized Pomeron propagator

$$\frac{1}{t - m_g^2} \to \frac{-\alpha_c'}{2} \frac{\Gamma[-\chi]\Gamma[1 - \frac{\alpha_c(t)}{2}]}{\Gamma[\frac{\alpha_c(t)}{2} - 1 - \chi]} e^{-i\pi\alpha_c(t)/2} \left(\frac{\alpha_c' s}{2}\right)^{\alpha_c(t)-2}. \tag{41}$$

The factors of $f(\epsilon_i)$ have indeed canceled. We can now find the full Pomeron contribution to proton-proton scattering by applying this same replacement rule to the graviton propagator in (29). The proton-proton differential cross section becomes

$$\frac{d\sigma}{dt} = \frac{\lambda^4 A^4(t) \Gamma^2[-\chi]\Gamma^2[1 - \frac{\alpha_c(t)}{2}]}{\pi\Gamma^2[\frac{\alpha_c(t)}{2} - 1 - \chi]} \left(\frac{\alpha_c' s}{2}\right)^{2\alpha_c(t)-2}, \tag{42}$$

corresponding to the invariant amplitude

$$\mathcal{A}(s, t) = 4s\lambda^2 A^2(t) e^{-i\pi\alpha_c(t)/2} \left(\frac{\Gamma[-\chi]\Gamma[1 - \frac{\alpha_c(t)}{2}]}{\Gamma[\frac{\alpha_c(t)}{2} - 1 - \chi]}\right) \times \left(\frac{\alpha_c' s}{2}\right)^{\alpha_c(t)-1}. \tag{43}$$

This form provides a model for the differential cross section, total cross section, and ρ parameter of either proton-proton or proton-antiproton scattering at very high center of mass energy, where the process is dominated by Pomeron exchange. This prediction is relatively model-independent, relying only on the structure of the closed string amplitude and the assumption that the graviton (which must be present in any dual theory) couples to the energy-momentum tensor. It depends on four parameters: the two trajectory parameters $\alpha_c(0)$ and α_c', the glueball-proton-proton coupling strength λ, and the dipole mass M_d (for small t we can approximate the form factor $A(t)$ with a dipole $A(t) = (1 - t/M_d^2)^{-2}$). Of these unknowns, the coupling λ, the dipole mass M_d, and the glueball mass $m_g^2 = (2 - \alpha_c(0))/\alpha_c'$ are all present in the low-energy process involving the exchange of the lowest glueball. That is, if we know the low-energy process, which we can compute in the supergravity limit, then the *only* dependence on the full string theory lies in determining the trajectory slope α_c'.

We now present two approaches for fixing the four parameters of the model: (1) we calculate three of them in a specific dual model, and (2) we compare these results to least-squares fits of our model to scattering data.

IV. COMPUTATION OF PARAMETERS IN THE SAKAI-SUGIMOTO MODEL

After briefly reviewing the Sakai-Sugimoto model [11], we compute the parameters m_g, λ, and M_d. We note first that the Sakai-Sugimoto model depends on three quantities, M_{KK}, g_{YM}, and l_s. The string scale l_s does not appear in the low-energy supergravity limit, only in the full string theory. The other two parameters are arbitrary *a priori*, but they may be fitted using the ρ mass and the pion decay constant [11]. We find excellent agreement between m_g, M_d, and λ as computed in the fully fixed Sakai-Sugimoto model, and the values determined by fitting to pp and $p\bar{p}$ scattering data.

A. Sakai-Sugimoto model

The Sakai-Sugimoto model [11,40], is a top-down QCD dual: it relies on a brane construction in 10-dimensional supergravity to produce the salient features of strongly coupled QCD, such as confinement and chiral symmetry breaking. N_f flavor $D8$-branes are placed in the background generated by N_c $D4$-branes. Closed string (or bulk) excitations are dual to QCD glueballs, while open strings living on the probe branes and transforming in the adjoint of a $U(N_f)$ symmetry are dual to scalar and vector mesons.

The $D4$ background is defined by the following metric, dilaton, and Ramond-Ramond three-form C_3 (with $F_4 = dC_3$):

$$\begin{aligned} ds^2 &= \left(\frac{U}{R}\right)^{3/2}(\eta_{\mu\nu}dx^\mu dx^\nu + f(U)d\tau^2) \\ &\quad + \left(\frac{R}{U}\right)^{3/2}\left(\frac{dU^2}{f(U)} + U^2 d\Omega_4^2\right), \\ e^\phi &= g_s\left(\frac{U}{R}\right)^{3/4}, \qquad F_4 = \frac{2\pi N_c}{V_4}\epsilon_4, \\ f(U) &\equiv 1 - \frac{U_{KK}^3}{U^3}. \end{aligned} \tag{44}$$

A radial coordinate U and a unit S^4 parametrize the directions transverse to the $D4$-branes. $d\Omega_4^2$ is the metric on the unit S^4, which has volume form ϵ_4 and volume $V_4 = 8\pi^2/3$. $R^3 = \pi g_s N_c l_s^3$. The $D4$-branes are extended in the τ and x^μ directions, for $\mu = 0, 1, 2, 3$. The τ direction is made periodic with $\tau \sim \tau + 2\pi M_{KK}^{-1}$. The radial coordinate U must now be bounded from below ($U \geq U_{KK}$) to avoid a conical singularity. In order to break the remaining supersymmetry, we impose antiperiodic boundary conditions on the fermionic modes so they acquire masses of order M_{KK}.

It is often useful to work with the scale and the effective four-dimensional coupling constant of the Yang-Mills theory. In terms of U_{KK} and R, $M_{KK} = 3U_{KK}^{1/2}/(2R^{3/2})$, and $g_{YM}^2 = 2\pi M_{KK} g_s l_s$.

Placing N_f $D8$-branes in this background produces flavor degrees of freedom (DOF). In the probe limit ($N_f \ll N_c$) the backreaction of the $D8$-branes with the $D4$-brane geometry is negligible. The flavor branes assume a nontrivial profile in the (U, τ) plane, and are fully extended along the x^μ and the S^4 directions.

B. Open and closed string spectra

Mass spectra of excitations coming from bulk and brane modes can be determined by perturbing the supergravity and the brane (Direc-Born-Infeld [DBI]) actions, respectively. Computations of the glueball (i.e. closed string) spectrum for this background geometry were performed in [41,42]. We briefly review the treatment of [41] using the conventions of [11], and cite relevant results.

The 10-dimensional bulk field content consists of the graviton, h_{MN}, a dilaton ϕ, an NS-NS tensor B_{MN}, and R-R one- and three-forms C_M and C_{MNL}. Neglecting any dependence on the S^4 transverse to the $D4$-branes, and ignoring all but the lowest KK modes in the compactified τ direction essentially reduces the problem to five dimensions: (x^μ, U). We can classify the states according to their transformation properties under $SO(3)$ rotations in the physical space directions (x_1, x_2, x_3) of the field theory. The graviton, in particular, gives rise to a 2^{++} state (h_{ij}), a 1^{-+} state ($h_{i\tau}$), and a 0^{++} state ($h_{\tau\tau}$). The coupling of the bulk fields to the boundary gauge theory and the parity- and charge-conjugation invariance of the overall action determine the parity and charge quantum numbers of the four-dimensional field theory states.

Now consider the standard supergravity action

$$S = \frac{1}{2\kappa_{10}^2}\int d^{10}x\sqrt{-G}\left\{e^{-2\phi}(R + 4(\nabla\phi)^2) - \frac{(2\pi)^4 l_s^6}{2\cdot 4!}F_4^2\right\}, \tag{45}$$

where κ_{10} is the 10-dimensional Newton constant. We introduce perturbations around the background metric by taking $G_{MN} = \tilde{G}_{MN} - h_{MN}$, where $\tilde{G}_{MN}$ is the background metric from Eq. (44). Varying with respect to h_{ij} (i, j are spatial Lorentz indices), we have the equations of motion

$$\begin{aligned} &-\frac{1}{2}\left(\frac{9f}{2} + 3Uf'\right)h_{ij} + (f + Uf')U\partial_U h_{ij} + fU^2\partial_U^2 h_{ij} \\ &= -\frac{q^2R^3}{U}h_{ij}. \end{aligned} \tag{46}$$

The prime denotes differentiation with respect to U, and q^2 is the four-dimensional momentum of the mode with $h_{ij}(q, U) = \int d^4x e^{-iqx}h_{ij}(x, U)$. We work in a gauge where $h_{0M} = 0$, $\partial_i h_{AB} = 0$ and retain the traceless (spin 2) piece of h_{ij}. Writing the 10-dimensional perturbation $h_{ij}(x, U)$ as a tower of resonances,

$$h_{ij}(x, U) = \sum_{n=1}^{\infty} h_{ij}^{(n)}(x)\left(\frac{U}{R}\right)^{3/2} T_n(U), \tag{47}$$

the equation of motion becomes an eigenvalue equation for the modes $T_n(U)$ with $q^2 = m_n^2$, where m_n is the mass of the nth resonance:

$$\partial_U(U^4 f \partial_U T_n) = -m_n^2 R^3 U T_n. \tag{48}$$

As discussed earlier, we work in a strict Regge limit, only taking into account contributions from the leading Regge trajectory, and not from the daughter trajectories. We will therefore use only the lightest mode in the KK tower of 2^{++} glueballs. For simplicity, we define $T(U) \equiv T_n(U)$, $h_{ij} \equiv h_{ij}^{(1)}$, and $m_g^2 \equiv m_1^2$ [43]. The mass of the lightest glueball is proportional to the lowest eigenvalue,

$$m_g^2 = 1.57 M_{KK}^2, \tag{49}$$

which agrees with the result derived in [41].

Having computed the mass of the lightest spin 2 graviton mode, we must now normalize its wave function to yield a canonical kinetic term in the effective four-dimensional action. The graviton kinetic term comes from

$$S = \frac{1}{2\kappa_{10}^2}\int d^{10}x\sqrt{-G}e^{-2\phi}R, \tag{50}$$

which we expand to quadratic order in $h_{\mu\nu}$:

$$\sqrt{-G}e^{-2\phi}R = \frac{1}{2}\sqrt{-\tilde{G}}e^{-2\tilde{\phi}}\tilde{G}^{\mu\nu}\tilde{G}^{\beta\delta}\tilde{G}^{\alpha\gamma} \times\left[\partial_\alpha h_{\delta\nu}\partial_\mu h_{\beta\gamma} - \frac{1}{2}\partial_\alpha h_{\delta\nu}\partial_\gamma h_{\beta\mu}\right] + \cdots, \tag{51}$$

assuming again that the graviton is traceless. Using the expansion in (47) and writing the integral in terms of the dimensionless ratio U/U_{KK},

$$S = \frac{N_c^3 M_{KK}^2 g_{YM}^2}{3^5\pi^2}\int_1^\infty \frac{U}{U_{KK}}T^2(U)d\left(\frac{U}{U_{KK}}\right)\int d^4x\frac{1}{2} \times \eta^{\mu\nu}\eta^{\beta\delta}\eta^{\alpha\gamma}\left[\partial_\alpha h_{\delta\nu}\partial_\mu h_{\beta\gamma} - \frac{1}{2}\partial_\alpha h_{\delta\nu}\partial_\gamma h_{\beta\mu}\right] + \cdots. \tag{52}$$

The coefficient of the kinetic term for the four-dimensional spin 2 mode is

$$\mathcal{N}_T^2 = \frac{N_c^3 M_{KK}^2 g_{YM}^2}{3^5\pi^2}\int_1^\infty \frac{U}{U_{KK}}T^2(U)d\left(\frac{U}{U_{KK}}\right) \equiv \frac{N_c^3 M_{KK}^2 g_{YM}^2}{3^5\pi^2}\mathcal{I}_T, \tag{53}$$

where $T(U)$ has dimensions of length and $\mathcal{I}_T$ has dimensions of length squared. Rescaling $T(U) \to T(U)/\mathcal{N}_T$ yields a canonically normalized kinetic term.

Now we turn to the open string spectrum on the $D8$-branes, given by the leading DBI action

$$S_{D8}^{\mathrm{DBI}} = -T_8\int d^9x e^{-\phi}\,\mathrm{tr}\sqrt{-\det(G_{MN} + 2\pi\alpha' F_{MN})}, \tag{54}$$

where $T_8 = (2\pi)^{-8}l_s^{-9}$ is the brane tension, G_{MN} is the pullback of the background metric onto the brane stack, and $F_{MN} = \partial_M A_N - \partial_N A_M - i[A_M, A_N]$ is the non-Abelian field strength of the $U(N_f)$ gauge fields living on the branes. We have used the convention $\mathrm{tr}(T^a T^b) = \delta^{ab}/2$ for the gauge group generators.

By extremizing the DBI action without gauge field fluctuations ($A_M = 0$), we can determine the profile of the $D8$-brane stack in the (U, τ) plane:

$$\tau(U) = \pm U_0^4 f(U_0)^{1/2} \times\int_{U_0}^{U}\frac{dU}{(\frac{U}{R})^{3/2}f(U)\sqrt{U^8 f(U) - U_0^8 f(U_0)}}, \tag{55}$$

where U_0 is a constant of integration. The geometry of the branes explicitly realizes chiral symmetry breaking. The radial coordinate U corresponds to the energy scale of the dual field theory. Near the UV boundary ($U \to \infty$), the solution exhibits chiral symmetry: it resembles a pair of parallel $D8$ and $\overline{D8}$ stacks separated in τ by some distance L, with four-dimensional modes transforming under $U(N_f)_L \times U(N_f)_R$. As U (the energy scale) decreases, the $D8$ and $\overline{D8}$ branes curve toward each other, until they meet at $U = U_0$, breaking the chiral symmetry of the two independent UV brane stacks to $U(N_f)_V$. Like [11], we focus on the solution where $U_0 = U_{KK}$, and the $D8$ and $\overline{D8}$ lie at antipodal points on the τ circle. It will prove convenient to parametrize the direction along the probe branes in (U, τ) plane with

$$Z = \pm\left[\left(\frac{U}{U_{KK}}\right)^3 - 1\right]^{1/2}, \tag{56}$$

where $Z \in (-\infty, \infty)$ such that $Z \to \pm\infty$ are the left (right) UV boundaries.

The gauge field fluctuations in the (μ, Z) directions on the $D8$-brane give rise to towers of four-dimensional vector and axial-vector meson states in the field theory. Assuming no dependence on the S^4 coordinates, the DBI action (54) becomes

$$S_{D8} = -\kappa\int d^4x dZ\,\mathrm{tr}\left[\frac{1}{2}K(Z)^{-1/3}\eta^{\mu\nu}\eta^{\rho\sigma}F_{\mu\rho}F_{\nu\sigma} + M_{KK}^2 K(Z)\eta^{\mu\nu}F_{\mu Z}F_{\nu Z} + \cdots\right], \tag{57}$$

with

$$\kappa = \frac{g_{YM}^2 N_c^2}{216\pi^3} \quad \text{and} \quad K(Z) = 1 + Z^2. \tag{58}$$

In order to ensure that the mass and kinetic terms of the four-dimensional action are normalizable, we must have the field strengths $(F_{\mu Z}, F_{\mu\nu}) \to 0$ as $Z \to \pm\infty$. We can choose a gauge where A_M itself vanishes at large Z. In order to more conveniently realize the (axial-)vector meson spectrum and the chiral Lagrangian for the pion modes, we follow [11] and transform to a gauge where $A_Z = 0$:

$$A_\mu(x^\mu, Z) \to A_\mu^{(g)} = gA_\mu g^{-1} + ig\partial_\mu g^{-1} \tag{59}$$

$$A_Z(x^\mu, Z) \to 0, \tag{60}$$

where the gauge transformation g has the form of a Wilson line,

$$g(x^\mu, Z) = P\exp\left[-i\int_0^Z dZ' A_Z(x^\mu, Z)\right]. \tag{61}$$

$A_\mu^{(g)}$ now splits naturally into a normalizable piece, $gA_\mu g^{-1}$, which gives rise to the (axial-)vector meson spectrum, and a non-normalizable piece $ig\partial_\mu g^{-1}$.

Focusing on the non-normalizable modes in the DBI action, we arrive at the action of the four-dimensional Skyrme model whose solitonic excitations we identify with baryons. The non-normalizable piece of $A_\mu^{(g)}$, $ig\partial_\mu g^{-1}$, changes the boundary conditions on the gauge field such that

$$\lim_{Z\to\pm\infty} A_\mu^{(g)}(x^\mu, \pm\infty) = \lim_{Z\to\pm\infty} ig\partial_\mu g \equiv i\xi_\pm(x^\mu)\partial_\mu\xi_\pm^{-1}(x^\mu), \tag{62}$$

where $\xi_+ \in U(N_f)_L$ and $\xi_- \in U(N_f)_R$. Imposing this behavior as a boundary condition, we can express $A_\mu^{(g)}$ as

$$A_\mu^{(g)} = i\xi_+\partial_\mu\xi_+\psi_+ + i\xi_-\partial_\mu\xi_-\psi_- + \sum_{n=1}^{\infty} B_\mu(x)^{(n)}\psi_n(Z) \tag{63}$$

with

$$\psi_\pm(Z) = \frac{1}{2}\left(1 \pm \frac{2}{\pi}\arctan(Z)\right). \tag{64}$$

The non-normalizable functions $\psi_\pm(Z)$ satisfy the gauge field equations of motion with boundary conditions $\psi_\pm(Z \to \pm\infty) = 1$ and $\psi_\pm(Z \to \mp\infty) = 0$. From $\xi_\pm(x^\mu)$ we can construct the appropriate chiral field $U(x^\mu) = \xi_+^{-1}\xi_-$ transforming as $U \to g_+ U g_-$ under $(g_+, g_-) \in U(N_f)_L \times U(N_f)_R$. Following [11], we use the residual gauge invariance to further fix $\xi_+ = U(x^\mu)$ and $\xi_- = 1$ so that

$$A_\mu^{(g)} = iU^\dagger\partial_\mu U\psi_+ + \text{normalizable modes}. \tag{65}$$

We have five-dimensional field strengths

$$F_{\mu\nu}^{(g)} = -[U^{-1}(x^\mu)\partial_\mu U(x^\mu), U^{-1}(x^\mu)\partial_\nu U(x^\mu)] \times \psi_+(\psi_+ - 1) \tag{66}$$

$$F_{Z\mu}^{(g)} = iU^{-1}(x^\mu)\partial_\mu U(x^\mu)\partial_Z\psi_+. \tag{67}$$

The DBI action now explicitly produces the four-dimensional Skyrme model

$$S_{\text{DBI}} = \kappa\int d^4x\,\text{tr}\{A(U^{-1}(x^\mu)\partial_\mu U(x^\mu))^2 + B[U^{-1}(x^\mu)\partial_\mu U(x^\mu), U^{-1}(x^\mu)\partial_\nu U(x^\mu)]^2\} \tag{68}$$

with parameters A and B defined by the overlap of the non-normalizable modes with warp factors associated with the background metric:

$$A = M_{KK}^2\int dZ(1+Z^2)(\partial_Z\psi_+)^2 = 0.318M_{KK}^2 \tag{69}$$

$$B = \frac{1}{2}\int dZ(1+Z^2)^{1/3}\psi_+^2(\psi_+ - 1)^2 = 0.078. \tag{70}$$

To match the Skyrme Lagrangian with $U(N_f)$ generators normalized to $\text{tr}(T^aT^b) = \delta^{ab}/2$,

$$S_{\text{Skyrme}} = \int d^4x\,\text{Tr}\left(\frac{f_\pi^2}{4}(U^{-1}\partial_\mu U)^2 + \frac{1}{32e^2}\times[U^{-1}\partial_\mu U, U^{-1}\partial_\nu U]^2\right) \tag{71}$$

we identify

$$f_\pi^2 = 4\kappa A \qquad \frac{1}{e^2} = 32\kappa B. \tag{72}$$

It is easy to show that taking $U(x^\mu) = \exp[-2i\pi(x^\mu)^a T^a/f_\pi]$ and expanding the action to leading order in the pion field indeed gives a canonical kinetic term for the pion. This is the form of the famous Skyrme model [44,45], in which baryons appear as solitonic configurations of $U(x^\mu)$. The second term in the Lagrangian (the "Skyrme term") stabilizes solitons of finite size. Including the ω meson and a gauged Wess-Zumino-Witten term can also be used for this purpose [46].

We are now in a position to fix the remaining free parameters from experimental data. Following [11], we use the ρ meson mass m_ρ to fix $M_{KK} = 949$ GeV and the pion decay constant $f_\pi = 93$ MeV to fix $\kappa = 7.45 \times 10^{-3}$ [47]. It should be noted that this is the crudest way to set the model parameters, and is intended only to yield a heuristic estimate of the values we can derive from the Sakai-Sugimoto model. More accurate results could be obtained by fitting to multiple real world parameters (such as several more [axial-]vector meson masses). An analysis of this type is conducted in the "hard-wall" model of [12].

C. Predictions for free parameters

Having detailed the various ingredients of the Sakai-Sugimoto gravity dual, we can now make predictions for three of the four parameters appearing in our ansatz for small t, large s proton-proton scattering: the ratio $-a_0/a'$, the dipole mass M_d in the gravitational form factor, and the coupling λ between the proton and the 2^{++} glueball. The first two quantities we take from the existing literature, and calculate the third directly.

(1) Using $M_{KK} = 949$ MeV and (49) we estimate $m_g \approx 1.49$ GeV. This value is significantly lower than the lattice result, $m_{g\text{-lattice}} = 2.40$ GeV [48]. In the next section, we find that our smaller value of m_g^2 more closely approximates the ratio $-a_0/a'$ we find by fitting our model to pp and $p\bar{p}$ scattering data.

(2) We model protons as four-dimensional Skyrmions, for which the matrix elements of the energy-momentum tensor (EMT) have been computed explicitly [38]. The form factors can be related to the components of the static EMT in Breit frame (that is with $k^0 = 0$):

$$T_{\mu\nu}(\mathbf{r}, \mathbf{s}) = \frac{1}{2p^0}\int \frac{d^3k}{(2\pi)^3} e^{i\mathbf{k}\cdot\mathbf{r}}\langle p', s'|T_{\mu\nu}(0)|p, s\rangle, \tag{73}$$

where the proton spin polarizations are defined to be equal in the respective protons' rest frames and equal to $s = (0, \mathbf{s})$. The form factors are given by

$$A(t) + B(t) + \frac{2t}{3}(A'(t) + B'(t)) = \int d^3\mathbf{r} e^{-i\mathbf{k}\cdot\mathbf{r}}\epsilon^{ijk}s_i r_j T_{\mathbf{r},\mathbf{s}} \tag{74}$$

$$A(t) + \frac{t}{4m^2}[A(t) + 2B(t) + 4C(t)] = \frac{1}{m}\int d^3\mathbf{r} e^{-i\mathbf{r}\cdot\mathbf{k}} T_{00}(\mathbf{r}, \mathbf{s}) \tag{75}$$

$$C'(t) + \frac{4t}{3}C'(t) + \frac{4t^2}{15}C''(t) = -\frac{m}{10}\int d^3\mathbf{r} e^{-i\mathbf{r}\cdot\mathbf{k}} T_{ij}(\mathbf{r})\left(r^i r^j - \frac{\mathbf{r}^2}{3}\delta^{ij}\right), \tag{76}$$

with m the nucleon mass, and primes denoting differentiation with respect to t. Evaluating the Skyrme EMT on the hedgehog solution of [45], $U = \exp[i\tau\cdot\hat{r}F(r)]$ with the radial function $F(r)$ chosen to minimize the soliton mass. Reference [38] determines the form factors explicitly in the large N_c limit. A dipole form approximates $A(t)$ well for up to $|t| < 0.8$ GeV^2, with dipole mass $M_d = 1.17$ GeV. This value for M_d is in good agreement with the value obtained by fitting to data, as presented in the next section.

A more rigorous analysis would treat the protons as five-dimensional solitons stabilized by vector mesons via the Chern-Simons term. This is beyond the scope of the present work and we take the ordinary four-dimensional Skyrme model to be sufficient to provide a heuristic estimate for M_d.

(3) We now compute the glueball-proton coupling in the Sakai-Sugimoto model, and find that the glueball indeed couples primarily to the four-dimensional energy-momentum tensor.

Let us consider graviton couplings in the DBI action, $h_{\mu\nu}$. Keeping only couplings linear in h,

$$\begin{aligned} S_{D8} &= -T_8\int d^9x e^{-\phi}\,\mathrm{tr}\sqrt{-\det(\tilde{G}_{MN} - h_{MN} + 2\pi\alpha' F_{MN})} \\ &= -\frac{1}{2}T_8(2\pi\alpha')^2\int d^9x e^{-\phi}\sqrt{\tilde{G}}\tilde{G}^{\mu\alpha}\tilde{G}^{\nu\beta}h_{\alpha\beta}(x, z)\,\mathrm{tr}(\tilde{G}^{\gamma\delta}F_{\mu\gamma}F_{\nu\delta} + \tilde{G}^{ZZ}F_{\mu z}F_{\nu z}) + \cdots \\ &= -\kappa\int d^4x h_{\alpha\beta}(x)\,\mathrm{tr}(A_h(U^{-1}\partial^\alpha U)(U^{-1}\partial^\beta U) + B_h[U^{-1}\partial^\alpha U, U^{-1}\partial_\rho U][U^{-1}\partial^\beta U, U^{-1}\partial^\rho U]) + \cdots \\ &\equiv -h_{\alpha\beta}C^{\alpha\beta} + \cdots. \end{aligned} \tag{77}$$

To arrive at the third line, we inserted the expressions for the field strengths in terms of $U(x)$ [Eq. (66)], and $h_{\alpha\beta}(x, Z)$, the pullback of the lightest graviton mode onto the branes. The coefficients A_h and B_h are given by the overlap integrals

$$A_h = \frac{18\sqrt{3}\pi M_{KK}}{N_c^{3/2}g_{YM}}\int_{-\infty}^{\infty} dZK(Z)\frac{T(Z)}{\mathcal{I}_T}(\partial_Z\psi_+)^2 = 13.42\frac{M_{KK}}{g_{YM}N_c^{3/2}} \tag{78}$$

$$B_h = \frac{9\sqrt{3}\pi}{N_c^{3/2}g_{YM}M_{KK}}\int_{-\infty}^{\infty} dZK(Z)^{-1/3}\frac{T(Z)}{\mathcal{I}_T} \times \psi_+^2(\psi_+ - 1)^2 = 7.64\frac{1}{g_{YM}N_c^{3/2}M_{KK}}. \tag{79}$$

Let us compare the tensor $C^{\alpha\beta}$ in (77) to the EMT of the four-dimensional Skyrme model,

$$T_{\alpha\beta} = \kappa\,\mathrm{tr}\{A(U^{-1}\partial_\alpha U)(U^{-1}\partial_\beta U) + 2B[U^{-1}\partial_\alpha U, U^{-1}\partial_\rho U] \times [U^{-1}\partial_\beta U, U^{-1}\partial^\rho U]\}. \quad (80)$$

We can extract the coupling constant λ as the ratio of the coefficients of either of the two terms in $C_{\alpha\beta}$ and $T_{\alpha\beta}$, or some linear combination of both. For example we can consider

$$C^{\alpha\beta} = \frac{A_h}{A}T^{\alpha\beta} + \kappa\left(B_h - \frac{2BA_h}{A}\right) \times [U^{-1}\partial^\alpha U, U^{-1}\partial_\rho U][U^{-1}\partial^\beta U, U^{-1}\partial^\rho U], \quad (81)$$

where

$$\frac{A_h}{A} = 42.18\frac{1}{M_{KK}g_{YM}N_c^{3/2}} = 3.61\ \mathrm{GeV}^{-1} \quad (82)$$

$$\left(B_h - \frac{2BA_h}{A}\right) = 0.09\ \mathrm{GeV}^{-1}. \quad (83)$$

Or alternatively

$$C^{\alpha\beta} = \frac{B_h}{2B}T^{\alpha\beta} + \kappa\left(A_h - \frac{AB_h}{2B}\right)(U^{-1}\partial^\alpha U) \times (U^{-1}\partial^\beta U), \quad (84)$$

where

$$\frac{B_h}{2B} = 48.86\frac{1}{N_c^{3/2}g_{YM}M_{KK}} = 4.19\ \mathrm{GeV}^{-1} \quad (85)$$

$$\left(A_h - \frac{AB_h}{2B}\right) = -0.17\ \mathrm{GeV}. \quad (86)$$

Assuming the relative contributions of the two terms (kinetic and Skyrme) are of the same order, the deviation of $C_{\alpha\beta}$ from the EMT amounts to a few percent of the value of λ. We therefore estimate $\lambda \sim 3.9 \pm 0.3\ \mathrm{GeV}^{-1}$, in excellent agreement with the fits discussed in the next section. It should be kept in mind however that the Skyrme model itself is only accurate to within ~20% so the value of λ derived from the Skyrme model may deviate from its actual value by somewhat more than this estimate.

V. DATA FITTING AND COMPARISON

A. Regime of validity

Before using our model to fit experimental scattering data, we briefly discuss the data we use, and limitations in applicability of our model as a function of s and t. We fit the differential cross section $d\sigma/dt$ for a variety of values of s and t (shown in Fig. 2). There are many complicating factors which limit the validity of our model, the most obvious being that we have worked in the strict Regge limit, neglecting corrections suppressed by powers of t/s. For all of the data we use, $t/s < 0.001$. Other effects, such as Coulomb contributions, perturbative QCD effects, and the contribution of Reggeon trajectories are not so easily discarded. We discuss each of these in some detail below.

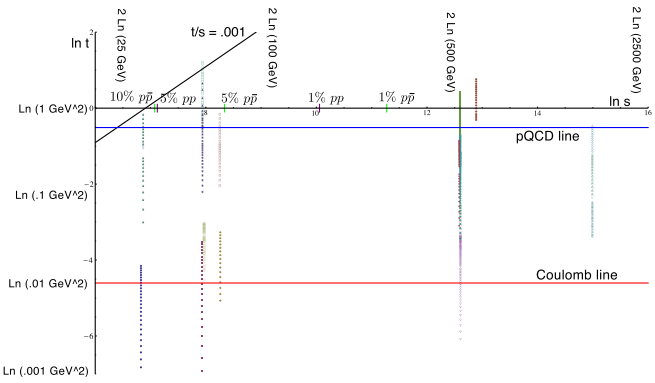

FIG. 2 (color online). Data from proton-proton and proton-antiproton scattering, with a dot for every data point in $(\log s, \log t)$ space. A given experiment is generally run at fixed s, for a range of values of t, so it creates a vertical series of data points. Below the diagonal line t/s corrections make up less than 0.1%. The horizontal line near the bottom lies at $|t| = 0.01\ \mathrm{GeV}^2$, which we are using as a lower cutoff. Below this line there are significant effects from Coulomb scattering. The horizontal line near the top is at $|t| = 0.6\ \mathrm{GeV}^2$, which we use as an upper cutoff. Along the log$s$ axis we mark the values at which the Reggeon contribution to proton-proton or proton-antiproton scattering is 1%, 5%, and 10%.

1. Coulomb contributions

For very small values of $|t|$ (regardless of s) the Coulomb interaction makes a significant contribution to the amplitude. This contribution will be largest at $|t| \simeq 0.002\ \mathrm{GeV}^2$ and is negligible (for our purposes) by $t \simeq 0.01\ \mathrm{GeV}^2$ [49,50]. We will use $|t| = 0.01\ \mathrm{GeV}^2$ as a lower cutoff in t.

2. Lower Regge trajectories

For large values of s, the total cross sections converge because the exchange of a Pomeron does not distinguish between particles and antiparticles. For small values of s, however, there are contributions to both proton-proton and proton-antiproton scattering from other Regge trajectories. In particular, the lower Regge trajectory is actually a pair of exchange degenerate trajectories, one consisting of even spin particles and the other of odd spin particles. For proton-antiproton scattering the Reggeon contribution is larger because these two trajectories add, whereas for proton-proton scattering they work to cancel each other out. We can estimate how large the contributions from the

next Regge trajectory will be by looking at the total cross sections for proton-proton and proton-antiproton scattering.

We fit the total cross sections shown in Fig. 3 with the functions

$$\sigma_{\rm tot}(pp \to pp) = Ps^p + Qs^q \tag{87}$$

$$\sigma_{\rm tot}(p\bar{p} \to p\bar{p}) = Ps^p + Rs^q \tag{88}$$

and find best-fit values

$$p = 0.08, \qquad q = -0.46, \qquad P = 21.3, \qquad Q = 53.2, \qquad R = 103.6. \tag{89}$$

We can use the optical theorem to relate the total cross section to the differential cross section at $t = 0$, and use this in turn to estimate the size of the first contribution from the lower trajectory.

$$\frac{d\sigma}{dt}(pp(p\bar{p})) \sim P^2 s^{2p}\left(1 + \frac{2Q(R)}{P} s^{q-p} + \cdots\right). \tag{90}$$

Based on this functional form, the magnitude of Reggeon contamination in proton-antiproton scattering at $\sqrt{s} = 31$ GeV is about 22%, while at $\sqrt{s} = 1800$ GeV it is about 0.3%. In Fig. 2, the marks on the log$s$ axis show where Reggeon contamination to proton-antiproton and proton-proton scattering is 1%, 5%, and 10%. For the lower center of mass energy data, the effect is fairly large. We could account for this by adding to our model a term corresponding to Reggeon exchange. For the present treatment, however, we simply add the amount of Reggeon contamination for a given value of s to the experimental error associated with each data point, thus weighting our fit toward the higher energy data.

3. Perturbative QCD and the hard Pomeron

For sufficiently small values of $|t|$, it is reasonable to think of the Pomeron as a trajectory of confined states (glueballs). This is the "soft Pomeron" on which our model is based. As $|t|$ increases, however, we eventually enter the regime of perturbative QCD, outside our model's regime of validity. It is not clear on theoretical grounds exactly where this transition occurs; we instead attempt to determine its location empirically, by examining the data. Let us assume that the Pomeron contribution to the differential cross section is of the form

$$\frac{d\sigma}{dt} = F(t)s^{2\alpha_c(t)-2} \tag{91}$$

for all values of t, where $F(t)$ is some unknown function. Differential cross section data are typically analyzed for a range of t values at a fixed value of s. Suppose instead we consider a fixed value of t for a range of values of s. The trajectory $\alpha_c(t)$ is therefore the slope of $\log(d\sigma/dt)$ plotted as a function of $\log(s)$:

$$\log\frac{d\sigma}{dt} = \log F(t) + (2\alpha_c(t) - 2)\log s. \tag{92}$$

By fitting for the slope of this line at a range of values of t, we can get a reasonable picture of the function $\alpha_c(t)$. Referring again to Fig. 2, we can see that taking sets of the data at fixed values of $|t|$ is difficult with the extant data, and generally these sets will only have between 3 and 5 data points each. This grouping of the data would not yield reliable statistics, so we do not use it to fit $\alpha_c(t)$ directly, but consider it a reasonable estimate of where the transition occurs between the regime where the soft Pomeron accurately characterizes the exchanged degrees of freedom, and the regime where it does not. A graph of $\alpha_c(t)$ as a function of $|t|$ is shown in Fig. 4. We can see that for $0 \le |t| \le 0.6$ GeV^2 the trajectory matches what we

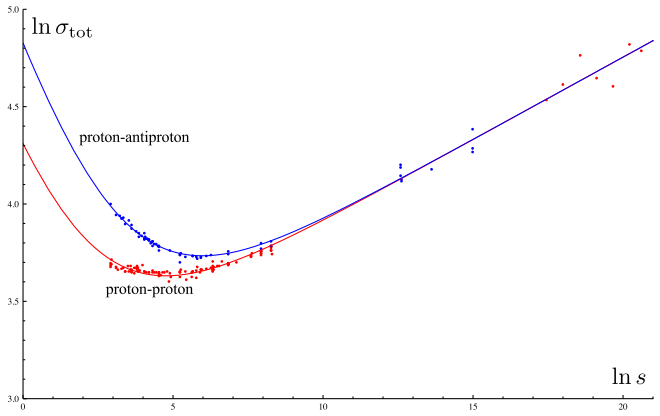

FIG. 3 (color online). Log-log plot of total cross sections (in mb) for proton-proton and proton-antiproton scattering as a function of s (in GeV^2). Note that the cross sections converge as s grows large.

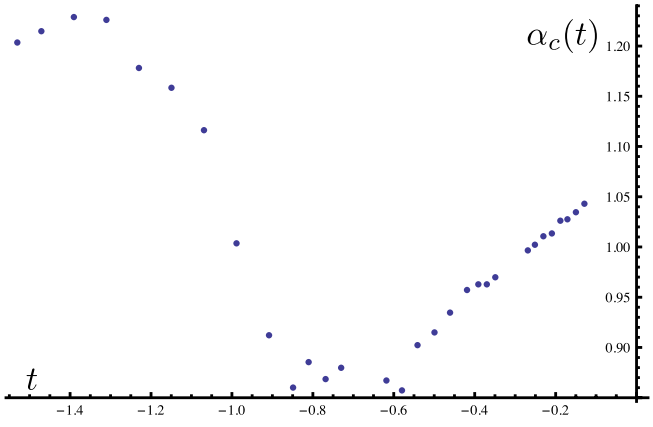

FIG. 4 (color online). The function $\alpha_c(t)$. In the region $0 \le |t| \le 0.6$ GeV^2 the trajectory matches that of the soft Pomeron. Outside this region we assume that perturbative QCD effects make our treatment inapplicable.

expect for the soft Pomeron. There is a clear transition at $|t| = 0.6$ GeV^2, where the slope suddenly becomes much less steep; above $|t| > 0.9$ GeV^2 the behavior is clearly nonlinear. We therefore attach no particular significance to the shape of the plot in this region, choosing instead to impose an upper bound of 0.6 GeV^2 on the values of $|t|$ we consider in our fits.

B. Comparison to a "Photo-Pomeron" model

In order to provide a frame of reference for the success of the model described above compared to the existing literature, we briefly review a commonly used model for single Pomeron exchange due to Donnachie, Jaroszkiewicz, Landshoff, Polkinghorne, and others [51–53]. This is only one of many possible models of various degrees of complication, but serves as an illustrative example because it has the same structure as our model, with the difference that it relies on the electromagnetic proton form factor rather than the gravitational form factor. Other models based on different assumptions include the impact picture model of [54], the multicomponent model of the Durham group (see [55,56] for a recent discussion) and the eikonal model of Block, Halzen, and collaborators (see e.g. [57] and references therein).

The electromagnetic-type Pomeron coupling (reviewed in [58]) draws inspiration from the additive quark rule: the (experimental) fact that the ratios of total cross section equal the ratios of the numbers of valence quarks present in the scattered hadrons. Positing that the Pomeron couples to constituent quarks individually as γ^μ reproduces this observation. The form of the Pomeron-quark coupling is then assumed to be identical to the photon coupling except that the Pomeron is $C = +1$ rather than $C = -1$. The form factor $F_1(t)$ involved in the exchange is assumed to be identical to the electromagnetic form factor. For $|t| < 1$ GeV^2, a dipole approximation to $F_1(t)$ (from electron scattering data) gives

$$F_1(t) = \frac{4m_p^2 - 2.79t}{4m_p^2 - t}\frac{1}{(1 - t/0.71)^2}. \tag{93}$$

Using this single-Pomeron exchange model, the unpolarized pp (or $p\bar{p}$) cross section becomes

$$\frac{d\sigma}{dt} = \frac{(3\beta_P F_1(t))^4}{4\pi}\left(\frac{s}{s_0}\right)^{2\alpha_P(t)-2}, \tag{94}$$

with $s_0 \approx 1$ GeV^2 the characteristic scale of the problem. The key difference between this model and ours lies in the form factor: gravitational in our case, electromagnetic in the case of the photo-Pomeron.

C. Fits to scattering data

We perform standard least-squares fits [59] to the differential cross section data for pp and $p\bar{p}$ scattering using the form (42), allowing the parameters α_0, α', M_d, and λ to vary. We also perform an identical fit for the photo-Pomeron model, allowing β_P, α_0 and α' to vary. The data are taken from the Durham high-energy physics database [60] with $0.01 < t < 0.6$ GeV^2 and $30.4 < \sqrt{s} < 1800$ GeV. As our model does not take into account the effects of Reggeon exchange, we simply estimate the contribution of Reggeons to $d\sigma/dt$ at particular values of $\sqrt{s}$, and add the result in quadrature to the experimental errors. There is significant disagreement between two data sets at $\sqrt{s} = 1800$ GeV produced by the CDF and E710 experiments, as shown in Fig. 5. Rather than choosing one or the other set explicitly, we perform all fits using both, just CDF, and just E710, with results as displayed in Table I.

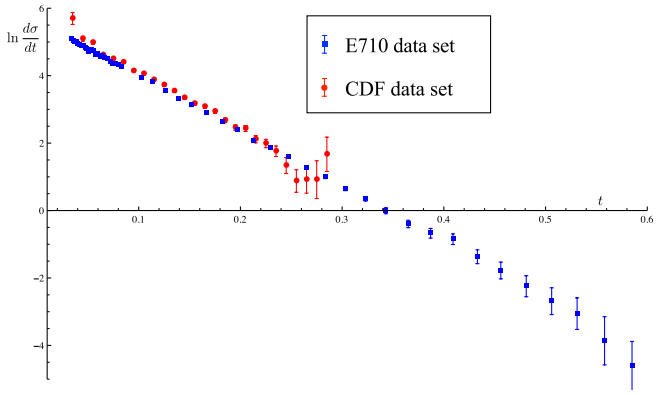

FIG. 5 (color online). A log-linear plot of the differential cross section at $\sqrt{s} = 1800$ GeV from the CDF and E710 collaborations, as a function of t (in GeV^2).

Our model clearly produces the smallest value of χ^2/DOF when only the CDF data set is included, but fares better than the photo-Pomeron model in all cases. Figure 6 shows fits of our model to the differential cross section data.

We can also compare our predictions for the total cross section and $\rho = \mathrm{Re}\mathcal{A}(t = 0)/\mathrm{Im}\mathcal{A}(t = 0)$ (based on the best-fit parameters determined from the differential cross section) to data. Applying the optical theorem to Eq. (40) yields the total cross section

$$\sigma_{\mathrm{tot}} = \frac{4\pi\lambda^2\Gamma[-\chi]}{\Gamma[\frac{\alpha_c(0)}{2}]\Gamma[\frac{\alpha_c(0)}{2} - 1 - \chi]}\left(\frac{\alpha_c' s}{2}\right)^{\alpha_c(0)-1} \equiv Cs^{\alpha_0 - 1}, \tag{95}$$

where in terms of the best-fit parameters (using only CDF data) we find $C = 21.325$ and $\alpha_0 - 1 = 0.085$. Performing an explicit χ^2 fit to total cross section data, we find $C_{\mathrm{fit}} = 21.097$ and $(\alpha_c(0) - 1)_{\mathrm{fit}} = 0.086$, in excellent agreement with the computation.

Because we neglect Reggeons, (40) predicts a constant value for ρ as $\rho = -\cot(\frac{\pi\alpha_0}{2} - \pi) = 0.136$ (where again we use the values of the best-fit parameters from the differential cross section). This value agrees well with the data at large $\sqrt{s}$ (see Fig. 7), where the Reggeon contribution is minimal.

TABLE I. Fits to differential cross section data including both E710 and CDF $\sqrt{s} = 1800$ data sets, just E710, or just CDF.

Gravitationally coupled Pomeron		
Both data sets	Just E710	Just CDF
$\alpha_c(0) = 1.076 \pm 0.0016$	$\alpha_c(0) = 1.074 \pm 0.0016$	$\alpha_c(0) = 1.086 \pm 0.0016$
$\alpha_c' = 0.290 \pm 0.006\ \mathrm{GeV}^{-2}$	$\alpha_c' = 0.286 \pm 0.006\ \mathrm{GeV}^{-2}$	$\alpha_c' = 0.300 \pm 0.006\ \mathrm{GeV}^{-2}$
$M_d = 0.983 \pm 0.016$ GeV	$M_d = 0.970 \pm 0.016$ GeV	$M_d = 1.02 \pm 0.016$ GeV
$\lambda = 4.28 \pm 0.03\ \mathrm{GeV}^{-1}$	$\lambda = 4.31 \pm 0.03\ \mathrm{GeV}^{-1}$	$\lambda = 4.14 \pm 0.03\ \mathrm{GeV}^{-1}$
$\frac{\chi^2}{\mathrm{DOF}} = 1.65$	$\frac{\chi^2}{\mathrm{DOF}} = 1.41$	$\frac{\chi^2}{\mathrm{DOF}} = 1.26$
Electromagnetically coupled Pomeron		
Both data sets	Just E710	Just CDF
$\alpha_c(0) = 1.076 \pm 0.0013$	$\alpha_c(0) = 1.075 \pm 0.0013$	$\alpha_c(0) = 1.082 \pm 0.0018$
$\alpha_c' = 0.289 \pm 0.003\ \mathrm{GeV}^{-2}$	$\alpha_c' = 0.289 \pm 0.003\ \mathrm{GeV}^{-2}$	$\alpha_c' = 0.289 \pm 0.003\ \mathrm{GeV}^{-2}$
$\beta = 1.858 \pm 0.016\ \mathrm{GeV}^{-1}$	$\beta = 1.877 \pm 0.016\ \mathrm{GeV}^{-1}$	$\beta = 1.801 \pm 0.020\ \mathrm{GeV}^{-1}$
$\frac{\chi^2}{\mathrm{DOF}} = 1.97$	$\frac{\chi^2}{\mathrm{DOF}} = 1.66$	$\frac{\chi^2}{\mathrm{DOF}} = 1.79$

We have shown that our mechanism for Pomeron exchange in pp and $p\bar{p}$ scattering fits experimental data quite well. The best-fit parameters from fitting the data also compare favorably with our estimates for $a_c(0)/a_c'$, λ, and M_d computed in holographic QCD. The Sakai-Sugimoto model predicts the mass of the lightest spin 2 glueball $m_g = 1.485$ GeV, while the value produced by fitting the form of the differential cross section to scattering data yields $m_{g\text{-fit}} = 1.745 \pm 0.035$ GeV, is within 15% of the computed mass, though not with the statistical error bars determined by the fit. The gravitational dipole mass M_d computed in the Skyrme model has value $M_d = 1.17$ GeV, which deviates from the fitted value $M_{d\text{-fit}} = 1.02 \pm 0.016$ by about 15% as well. As the Skyrme model predicts masses only to an accuracy of about 20%, the fitted value lies within the expected uncertainty of the computed dipole mass. Finally, the coupling constant computed from holography to be $\lambda \approx 3.90 \pm 0.3\ \mathrm{GeV}^{-1}$ agrees extremely well with the best-fit value of $4.14 \pm 0.04\ \mathrm{GeV}^{-1}$.

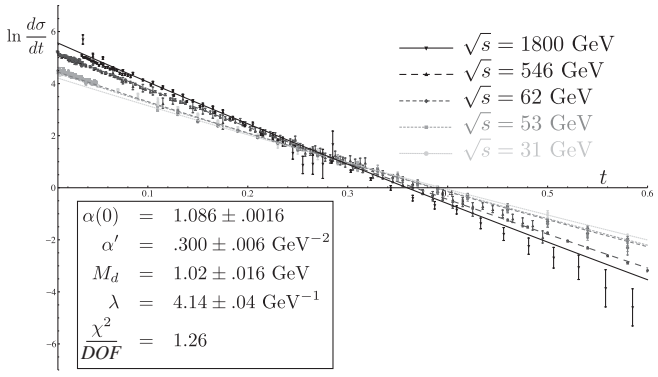

FIG. 6. A log-linear plot of the best-fit to the scattering data using just the CDF data at $\sqrt{s} = 1800$ GeV. The differential cross section is in mb/GeV^2 and t is in GeV^2. Note that at lower center-of-mass energies the fit is less successful, most likely due to a greater contribution from Reggeon exchange.

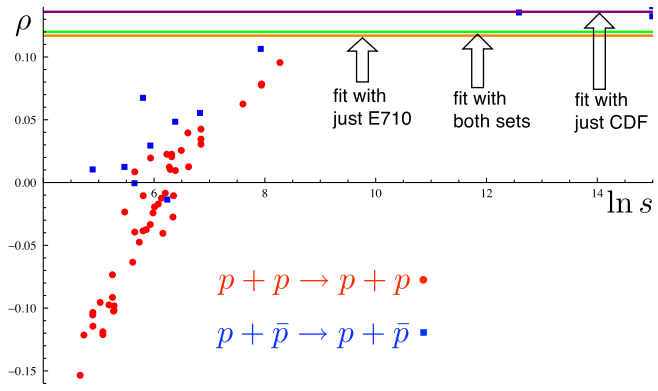

FIG. 7 (color online). Data for ρ as a function of log$s$ compared to the predicted value.

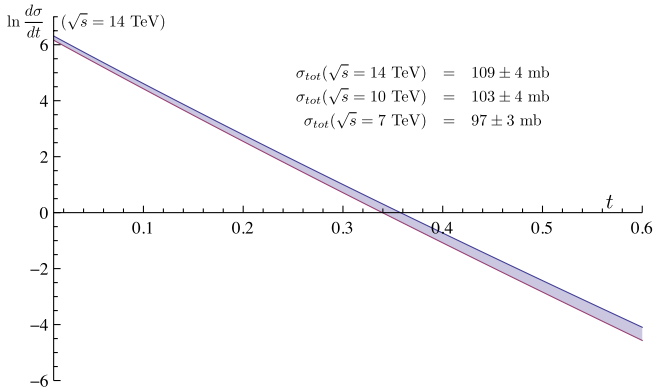

FIG. 8 (color online). A log-linear plot of the predicted LHC differential cross section (in mb/GeV^2) as a function of t (in GeV^2) at $\sqrt{s} = 14$ TeV. We have used the best-fit parameters from the data set including only the CDF $\sqrt{s} = 1800$ GeV data. The range shown is generated by the errors in the fit parameters.

We should note that the values of χ^2 per DOF we obtain are not as good as those of fits cited in the current Particle Data Group values which typically fit to a leading $\log^2 s$ behavior and use more sophisticated filtering of the data than we have done [61–63].

Finally, we can use our model for pp scattering to make a prediction for the differential and total cross sections to be observed at the LHC (at $\sqrt{s} = 14$ TeV). The differential cross section $d\sigma/dt$ is plotted in Fig. 8 as a function of the momentum transfer, t. We predict a total cross section of $\sigma_{\text{tot}} = 109 \pm 4$ mb.

VI. CONCLUSIONS AND FUTURE DIRECTIONS

We have used AdS/QCD to construct a general model for Pomeron exchange in Regge-limit pp and $\bar{p}p$ scattering. In order to do so, we assumed that string scattering amplitudes have the same structure in weakly curved space as they do in flat space, but that the *values* of the Regge trajectory parameters and the masses of excitations are modified. This implies that the curved space Regge regime amplitude factorizes into a piece that characterizes the interaction of the scattered particles with the exchanged trajectory, and a piece that corresponds simply to the exchange of a closed string (the Reggeized propagator). Furthermore, the coupling of the external states to the exchanged trajectory is described entirely by their coupling to the lowest mode (the 2^{++} glueball).

Using these principles, and generic properties of QCD duals, we were able to identify the form factor $A(t)$ at the Pomeron-proton vertex as coming from the matrix element of the energy-momentum tensor, with the strength of the coupling given by an overlap of graviton and pion wave functions. In a particular hQCD dual, the Sakai-Sugimoto model, we computed the coupling directly and showed that it agrees with one determined by fits to experimental data. We also developed a method for extending the amplitude for exchanging the 2^{++} glueball to include the exchange of the entire glueball trajectory.

Though our treatment offers several advantages compared to previous approaches to this problem, there are some ways in which our methodology could be improved or extended. At the level of numerical analysis, our errors did not take into account systematic errors that might drive an entire data set at a particular $\sqrt{s}$ either up or down. More sophisticated fitting techniques would also filter outliers out of the data, which could significantly improve the χ^2 we find.

On a theoretical level, one could certainly extend the regime of validity of our model to lower values of $\sqrt{s}$ by modeling Reggeon (open string) exchange as well as Pomeron exchange. Our treatment of the proton in the dual model was also rather simplistic. Computing the proton form factors and proton-proton-glueball coupling using the duals of baryons as five-dimensional instantons in the Sakai-Sugimoto model [64,65] rather than via the simple four-dimensional Skyrme model, would yield a more accurate holographic picture; one should also take into account that the five-dimensional solitons may be stabilized using vector meson modes. As mentioned above, [35] recently presented a treatment of protons as fermionic fields in bottom-up holographic models, which included results for the electromagnetic and gravitational form factors. It would be interesting to incorporate these techniques, possibly coupled with the Skyrmion picture of protons, into our model.

We used the four-point sphere amplitude to model the Reggeized propagator. In the Regge limit this amplitude indeed consists of the t-channel exchange of a closed string, to which the Pomeron is dual. However, it is not clear that the incoming and outgoing particles (the protons) are themselves dual to closed strings. As they may be considered as either to solitonic configurations of open string modes (pions) or as wrapped $D4$-branes, we might need to consider a more complicated amplitude to accurately reflect the structure of the scattering process. This is a difficult problem, but additional insight might be gained from π-π scattering, where the string dual should be an annulus amplitude.

Finally, there is the difficult issue of corrections for large s. The Froissart bound indicates that at some high s, the behavior $s^{\alpha(0)-1}$ for the total cross section must be replaced by a function that grows at most like $\log^2 s$. There are two possible sources for large s corrections to our model: string loop corrections, also known as Regge cuts or multiple Pomeron exchange, and corrections to the string amplitude from the curvature of the AdS space. It is certainly possible that such effects already play a role at energies we consider. More thoroughly examining the effects of spacetime curvature, in particular, would improve the accuracy of our predictions, and would hopefully serve as evidence for the existence of a curved-space string dual to QCD.

ACKNOWLEDGMENTS

This work was supported in part by NSF Grants PHY-00506630 and 0529954 and DOE Grant 580093. We thank Jon Rosner for helpful conversations. S. D. and N. M. would like to thank Alison Brizius for numerical assistance. J. H, N. M, and S. D. acknowledge the Galileo Galilei Institute for Theoretical Physics, the Kavli Institute for Theoretical Physics, and Imperial College London, respectively, for hospitality during the course of this work.

[1] For unpolarized scattering these quantities should be averaged over initial spins.
[2] A. V. Manohar, arXiv:hep-ph/9802419.
[3] S. R. Coleman, in *Aspects of Symmetry: Selected Erice Lectures* (Cambridge University Press, Cambridge, England, 1985).
[4] P. D. B. Collins, *An Introduction To Regge Theory and High-Energy Physics* (Cambridge University, Cambridge, England, 1977).
[5] G. F. Chew and S. C. Frautschi, Phys. Rev. Lett. **7**, 394 (1961).
[6] V. N. Gribov, Sov. Phys. JETP **14**, 478 (1961).
[7] P. D. B. Collins, F. D. Gault, and A. D. Martin, Nucl. Phys. **B80**, 135 (1974).
[8] A. Donnachie and P. V. Landshoff, Phys. Lett. B **296**, 227 (1992).
[9] J. R. Cudell, V. Ezhela, K. Kang, S. Lugovsky, and N. Tkachenko, Phys. Rev. D **61**, 034019 (2000); **63**, 059901 (E) (2001).
[10] E. Witten, Adv. Theor. Math. Phys. **2**, 505 (1998).
[11] T. Sakai and S. Sugimoto, Prog. Theor. Phys. **113**, 843 (2005).
[12] J. Erlich, E. Katz, D. T. Son, and M. A. Stephanov, Phys. Rev. Lett. **95**, 261602 (2005).
[13] L. Da Rold and A. Pomarol, Nucl. Phys. **B721**, 79 (2005).
[14] J. M. Maldacena, Adv. Theor. Math. Phys. **2**, 231 (1998); Int. J. Theor. Phys. **38**, 1113 (1999).
[15] S. S. Gubser, I. R. Klebanov, and A. M. Polyakov, Phys. Lett. B **428**, 105 (1998).
[16] E. Witten, Adv. Theor. Math. Phys. **2**, 253 (1998).
[17] R. C. Brower, J. Polchinski, M. J. Strassler, and C. I. Tan, J. High Energy Phys. 12 (2007) 005.
[18] C. Csaki, H. Ooguri, Y. Oz, and J. Terning, J. High Energy Phys. 01 (1999) 017; R. de Mello Koch, A. Jevicki, M. Mihailescu, and J. P. Nunes, Phys. Rev. D **58**, 105009 (1998); R. C. Brower, S. D. Mathur, and C. I. Tan, Nucl. Phys. **B587**, 249 (2000).
[19] H. B. Meyer and M. J. Teper, Phys. Lett. B **605**, 344 (2005).
[20] For an introduction see J. R. Forshaw and D. A. Ross, *Quantum Chromodynamics and the Pomeron* (Cambridge University Press, Cambridge, England, 1997).
[21] A. M. Polyakov, Nucl. Phys. B, Proc. Suppl. **68**, 1 (1998).
[22] O. Andreev, Phys. Rev. D **71**, 066006 (2005).
[23] O. Andreev and W. Siegel, Phys. Rev. D **71**, 086001 (2005).
[24] R. A. Janik, Phys. Lett. B **500**, 118 (2001).
[25] G. Veneziano, Nuovo Cimento A **57**, 190 (1968).
[26] C. Lovelace, Phys. Lett. B **28**, 264 (1968).
[27] J. A. Shapiro, Phys. Rev. **179**, 1345 (1969).
[28] E. Witten, Nucl. Phys. **B160**, 57 (1979).
[29] P. G. O. Freund, Phys. Lett. **2**, 136 (1962).
[30] P. G. O. Freund, Phys. Rev. Lett. **16**, 291 (1966).
[31] H. Pagels, Phys. Rev. **144**, 1250 (1966).
[32] S. J. Brodsky and G. F. de Teramond, Phys. Rev. D **78**, 025032 (2008).
[33] X. D. Ji, Phys. Rev. D **55**, 7114 (1997).
[34] E. Witten, J. High Energy Phys. 07 (1998) 006.
[35] Z. Abidin and C. E. Carlson, Phys. Rev. D **79**, 115003 (2009).
[36] S. Hong, S. Yoon, and M. J. Strassler, J. High Energy Phys. 04 (2006) 003.
[37] H. R. Grigoryan and A. V. Radyushkin, Phys. Lett. B **650**, 421 (2007).
[38] C. Cebulla, K. Goeke, J. Ossmann, and P. Schweitzer, Nucl. Phys. **A794**, 87 (2007).
[39] M. Yamada, Phys. Rev. D **30**, 2144 (1984).
[40] T. Sakai and S. Sugimoto, Prog. Theor. Phys. **114**, 1083 (2005).
[41] R. C. Brower, S. D. Mathur, and C. I. Tan, Nucl. Phys. **B587**, 249 (2000).
[42] N. R. Constable and R. C. Myers, J. High Energy Phys. 10 (1999) 037.
[43] Note that there is an additional KK tower due to excitations in the compact τ direction. Again, we are only interested in the lightest mode, so we assume that h_{ij} also has zero momentum in the τ direction.
[44] G. S. Adkins, C. R. Nappi, and E. Witten, Nucl. Phys. **B228**, 552 (1983).
[45] T. H. R. Skyrme, Proc. R. Soc. A **260**, 127 (1961).
[46] G. S. Adkins and C. R. Nappi, Phys. Lett. **137B**, 251 (1984).
[47] The string length l_s remains a free parameter, but none of the quantities relevant to the present analysis depend on it directly.
[48] C. J. Morningstar and M. J. Peardon, Phys. Rev. D **60**, 034509 (1999).
[49] N. A. Amos *et al.*, Nucl. Phys. **B262**, 689 (1985).
[50] D. Bernard *et al.* (UA4 Collaboration), Phys. Lett. B **198**, 583 (1987).
[51] A. Donnachie and P. V. Landshoff, Nucl. Phys. **B231**, 189 (1984).
[52] P. V. Landshoff and J. C. Polkinghorne, Phys. Rev. D **10**, 891 (1974).
[53] G. A. Jaroszkiewicz and P. V. Landshoff, Phys. Rev. D **10**, 170 (1974).
[54] C. Bourrely, J. Soffer, and T. T. Wu, Nucl. Phys. **B247**, 15 (1984).
[55] M. G. Ryskin, A. D. Martin, and V. A. Khoze, Eur. Phys. J. C **60**, 249 (2009).
[56] M. G. Ryskin, A. D. Martin, and V. A. Khoze, Eur. Phys. J. C **60**, 265 (2009).
[57] M. M. Block, E. M. Gregores, F. Halzen, and G. Pancheri, Phys. Rev. D **60**, 054024 (1999).
[58] A. Donnachie, H. G. Dosch, P. V. Landshoff, and O. Nachtmann, *Pomeron Physics and QCD* (Cambridge University Press, Cambridge, England, 2002).
[59] All fits are completed using PYTHON MINUIT.
[60] The Durham HEP Databases, http://durpdg.dur.ac.uk.
[61] J. R. Cudell *et al.*, Phys. Rev. D **65**, 074024 (2002).
[62] K. Igi and M. Ishida, Phys. Rev. D **66**, 034023 (2002).
[63] M. M. Block and F. Halzen, Phys. Rev. D **70**, 091901 (2004).
[64] H. Hata, T. Sakai, S. Sugimoto, and S. Yamato, Prog. Theor. Phys. **117**, 1157 (2007).
[65] K. Hashimoto, T. Sakai, and S. Sugimoto, Prog. Theor. Phys. **120**, 1093 (2008).